ACS OMEGA

Article

Cite This: ACS Omega 2020, 5, 877−881

http://pubs.acs.org/journal/acsodf

Selective Detection of Cu^{2+} Ions by Immobilizing Thiacalix[4]arene on Graphene Field-Effect Transistors

Yuki Takagiri, Takashi Ikuta,* and Kenzo Maehashi*

Institute of Engineering Tokyo University of Agriculture and Technology, 2-24-16, Nakacho, Koganei, Tokyo 184-8588, Japan

ABSTRACT: Highly accurate quantitative detection of heavy metals is essential for environmental pollution monitoring and health safety. Here, for selective detection of Cu^{2+} ions with high sensitivity, thiacalix[4]-arene (TCA) immobilized on graphene field-effect transistors (G-FETs) are developed. Our proposed TCA-immobilized G-FETs are successfully used to detect Cu^{2+} ions at concentrations ranging from 1 μM to 1 mM via changes in their transfer characteristics. Moreover, the measured transfer characteristics clearly shift only when Cu^{2+} ions are introduced in the buffer solution despite it containing other metal ions, including those of Na^{+}, Mg^{2+}, Ni^{2+}, and Cd^{2+}; this selective detection of Cu^{2+} ions is attributed to the planar arrangement of TCA on graphene. Therefore, TCA-immobilized G-FETs selectively detect Cu^{2+} with high sensitivity.

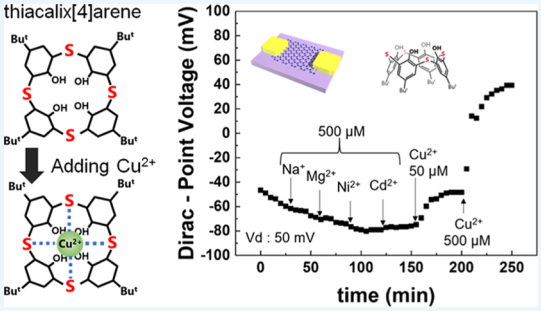

INTRODUCTION

Detection of heavy metal ions is necessary for environmental monitoring and health safety.[1] In the same vein, identification and quantification of heavy metal ions is crucial for determining water quality.[2−7] Currently, conventional analytical approaches such as atomic absorption spectrometry and inductively coupled plasma−mass spectrometry have been utilized in laboratory settings to identify and quantify heavy metal ions in environmental and biological samples.[8−12] However, these approaches are not suitable for onsite analysis of heavy metal concentrations owing to the size of the equipment used for them. In addition, heavy metal analysis is not straightforward owing to the complexity of the analytical processes and relatively long measurement times. Considering this, portable devices that can be used for highly sensitive onsite detection of heavy metal ions are needed. Thus, in this study, we developed graphene-based devices to achieve this.

Graphene is a one-atom-thick two-dimensional carbon sheet characterized by high carrier mobility and chemical stability, which can also be used for device miniaturization.[13,14] Owing to these properties, in recent times, graphene has attracted significant attention as a sensor material in sensor devices. An example of such a device is the graphene field-effect transistor (G-FET).[15−19] In particular, when charged molecules are adsorbed on graphene channels in G-FETs, the adsorbed molecules induce carriers on the graphene channels, resulting a shift in the charge neutrality point of G-FETs.[20] In addition, because of the high carrier mobility of graphene,[13,14] these shifts lead to significant changes in the drain current. Consequently, G-FETs can be used to detect molecules with high sensitivity. However, graphene alone cannot be used for selective detection of different target molecules. Therefore, to obtain selectivity, different types of receptors, such as antibodies, aptamers, enzymes, DNA, and supramolecules, immobilized on graphene have been used in previous studies.[20−29]

In this work, to achieve selectivity, we study the use of thiacalix[4]arene (TCA) as a receptor. TCA is composed of benzene rings linked via sulphide bridges;[30−33] it is known to form complexes with various heavy metal ions owing to its different conformations and the presence of bridging sulfur atoms.[34−37] The coordination between TCA and different heavy metal ions occurs through three-dimensional coordinated structures.[38−40] In particular, owing to its three-dimensional coordinated structure, TCA adsorbs several different heavy metal ions without selectivity. However, for selective detection of specific heavy metal ions, the coordination structure of metal ions needs to be modulated.

In our work, to realize selective detection of Cu^{2+}, planar-coordinated structures between TCA and Cu^{2+} were formed by immobilizing TCA on the surface of graphene. This immobilization occurs because of $\pi-\pi$ stacking between TCA and graphene, which limits the coordination forms of TCA.[41,42] Our analysis results revealed that TCA-immobilized G-FETs electrically responded to Cu^{2+} ions over a wide concentration range, thus demonstrating their potential utility for monitoring Cu^{2+} ion concentrations, despite the presence of various other metal ions in solutions.

RESULTS AND DISCUSSION

Detection of Cu^{2+} Ions Using TCA-Immobilized G-FETs. In this study, we demonstrated the detection of Cu^{2+} ions using TCA-immobilized G-FETs. Figure 1 shows the transfer characteristics of TCA-immobilized G-FETs before

Received: November 10, 2019
Accepted: December 12, 2019
Published: December 26, 2019

DOI: 10.1021/acsomega.9b03821
ACS Omega 2020, 5, 877−881

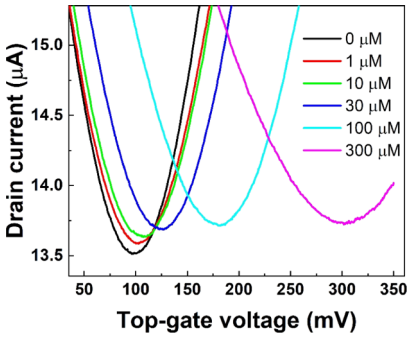

Figure 1. Transfer characteristics of the TCA-immobilized G-FET at different Cu^{2+} concentrations.

and after introducing Cu^{2+} ions at concentrations of 1, 10, 30, 100, and 300 μM. Bipolar characteristics were observed for the buffer solutions at all Cu^{2+} concentrations. Because the leakage current of G-FETs is 1000 times smaller than the drain current, the leakage current is negligible for detection of Cu^{2+}. The results revealed that the transfer characteristics shifted in the positive gate-voltage direction when Cu^{2+} ions are introduced, indicating that G-FETs can be used to detect Cu^{2+} ions based on these electrical measurement changes. Furthermore, the shifts in the transfer curves increased with increasing Cu^{2+} concentration; in particular, the shift at a Cu^{2+} concentration of 300 μM was as large as ~200 mV. Also, the average of the shifts at 300 μM was 186 ± 20 mV; the results indicated that G-FETs have repeatability for detection of Cu^{2+} ions. The observed positive shifts in Figure 1 were different from the results in a previous study that used G-FET-based sensors, wherein the accumulation of positive charges on graphene channels in G-FETs led to negative shifts in transfer curves.[43] In contrast, our results shown in Figure 1 imply that the charge distribution in TCA changed because of the formation of complexes between Cu^{2+} and TCA, as shown in Figure 2;[44−46] in turn, this change in the charge distribution induced potential changes in the graphene channel, resulting in the positive shift in transfer characteristics.

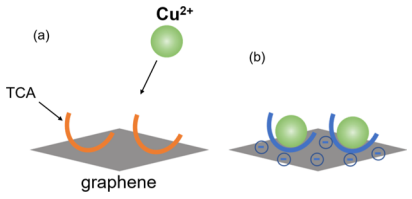

Figure 2. Schematic images of Cu^{2+} ions (a) before and (b) after coordinating with TCA.

Cu^{2+} Concentration Dependence. Next, the dependence of Cu^{2+} ion concentration on voltage characteristics of TCA-immobilized G-FETs was investigated. The transfer characteristics were measured every 5 min, and the Dirac-point voltage (V_{DP}) was plotted. Figure 3a shows the shifts in V_{DP} with time for various ion concentrations of Cu^{2+} ranging from 0 to 1 mM; the results shown in the figure reveal that the shift in V_{DP} increased with increasing Cu^{2+} ion concentration. Furthermore, change in V_{DP} almost stopped within 15 min at each Cu^{2+} concentration. This occurs because the adsorption of Cu^{2+} ions on TCA attains an equilibrium state. Therefore, G-FETs with TCA can be used to detect Cu^{2+} ions in a concentration range of 1 μM to 1 mM within 15 min. Figure

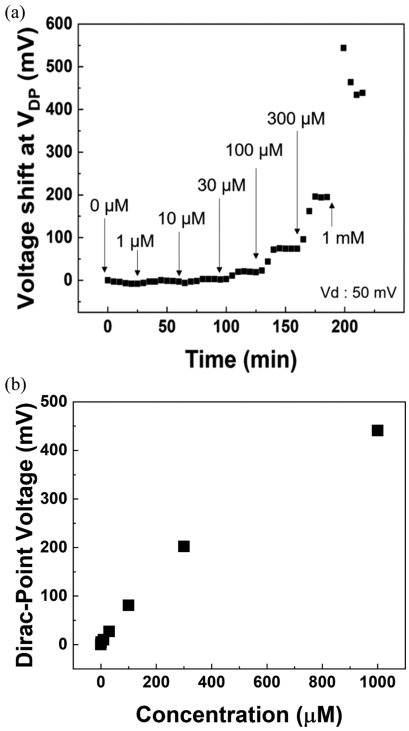

Figure 3. (a) Shifts in V_{DP} with time for various ion concentrations of Cu^{2+} and (b) shift in V_{DP} shift as a function of concentration of Cu^{2+} ranging from 0 to 1 mM.

3b shows the amount of V_{DP} shift as a function of concentration of Cu^{2+} ranging from 0 to 1 mM. The result reveals that the V_{DP} shift increases linearly with the concentration of Cu^{2+} ranging from 0 to 300 μM. On the other hand, the V_{DP} shift at 1 mM is slightly deviated from the linearity, indicating that the V_{DP} shift gradually saturated over 300 μM.

Selectivity of TCA-Immobilized G-FETs for Cu^{2+} Ions. To investigate the selectivity of TCA-immobilized G-FETs for Cu^{2+}, the shifts in V_{DP} were measured in Tris-HCl buffer containing other metal ions (Na^{+}, Mg^{2+}, Ni^{2+}, and Cd^{2+}). Figure 4a shows these shifts in V_{DP} when Na^{+}, Mg^{2+}, Ni^{2+}, and Cd^{2+} ions at concentrations of 500 μM each were sequentially added to the solution, after which Cu^{2+} ions at concentrations of 50 and 500 μM were added; the results show that V_{DP} did not clearly shift when Na^{+}, Mg^{2+}, Ni^{2+}, and Cd^{2+} ions were introduced in the solution. In contrast, a clear V_{DP} shift was observed when Cu^{2+} ions were introduced in the solution. Therefore, TCA-immobilized G-FETs showed selective detection of Cu^{2+} ions even in a solution containing other metal ions. Figure 4b shows the changes in V_{DP} for each metal ion (Na^{+}, Mg^{2+}, Ni^{2+}, Cd^{2+}, and Cu^{2+}) at concentrations of 500 μM in the form of a bar graph. In particular, the V_{DP} shift at 500 μM was observed to be over 100 mV for Cu^{2+} ions, which was more than 10 times larger than those recorded when Na^{+}, Mg^{2+}, Ni^{2+}, and Cd^{2+} ions were introduced. This selectivity for Cu^{2+} ions results from the immobilization of TCA on the graphene channel. The recognition of Cu^{2+} ions using TCA immobilized on graphene can be explained using the hard and soft acids and bases (HSAB) theory and the ligand field theory.[47,48] According to the HSAB theory, soft metal ions (Cu^{2+}, Ni^{2+}, and Cd^{2+}) tend to easily coordinate with sulfur atoms. Results from previous works indicate that TCA dispersed in solution captures not only Cu^{2+} ions, but also

DOI: 10.1021/acsomega.9b03821
ACS Omega 2020, 5, 877−881

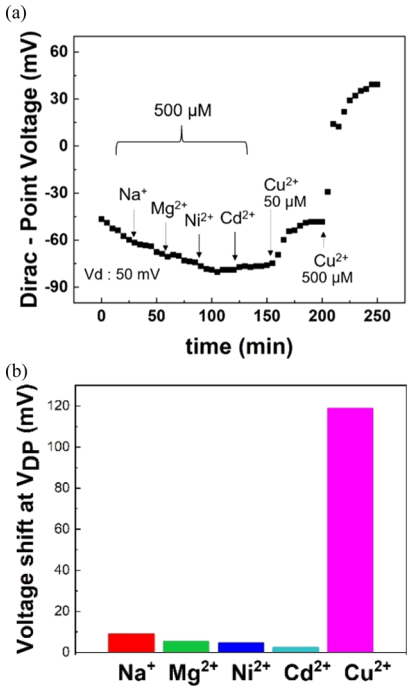

Figure 4. (a) V_{DP} as a function of time with other metal ions (Na^+, Mg^{2+}, Ni^{2+}, and Cd^{2+}) at 500 μM and Cu^{2+} at 50 and 500 μM. (b) Shifts in V_{DP} due to different metal ions (Na^+, Mg^{2+}, Ni^{2+}, Cd^{2+}, and Cu^{2+}) at 500 μM.

Ni^{2+} and Cd^{2+} ions through the liquid−liquid extraction method.[35,49] However, it is interesting to note that, compared with these previous works, our results indicate that TCA on the graphene surfaces capture only Cu^{2+} ions, which, in turn, implies that the space degrees of freedom of TCA were limited by immobilizing it on graphene surfaces. In particular, in the case of the liquid−liquid extraction method, the orientation and position of TCA changes relatively freely in solutions; consequently, several different heavy metal ions are surrounded by three TCA molecules leading to their adsorption.[35,49] However, when immobilized on G-FETs, TCA was planarly placed on the graphene surfaces; therefore, TCA cannot surround and adsorb several types of heavy metal ions when it is immobilized so. The coordination between Cu^{2+} ions and G-FETs occurs via the host−guest interaction. As depicted in Figure 5, Cu^{2+} ions are generally coordinated in a square shape,

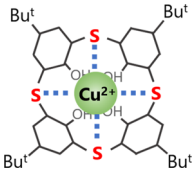

Figure 5. Coordination of TCA with Cu^{2+} ions.

as are the bridging sulfur atoms in TCA leading to the coordination of the bridging sulfur atoms with Cu^{2+} ions and their subsequent adsorption.[50] On the contrary, coordination forms of the other heavy metal ions are not of square type, but instead are of tetrahedron and octahedron types, which is why they do not coordinate with TCA immobilized on graphene.[51] In summary, the selectivity of G-FETs for Cu^{2+} ions is attributed to the immobilization of TCA on graphene surfaces in G-FETs. Therefore, G-FETs can be successfully used in the selective detection of Cu^{2+}.

CONCLUSIONS

In this study, we fabricated Cu^{2+} sensors using TCA-immobilized G-FETs. The transfer characteristics shifted in the positive gate-voltage direction on introducing Cu^{2+} ions in the solution; in addition, the V_{DP} shift increased as the Cu^{2+} concentration was increased from 1 μM to 1 mM, which indicates that G-FETs can be used for quantitative analysis of Cu^{2+}. Furthermore, TCA-immobilized G-FETs were able to successfully detect Cu^{2+} ions selectively in a buffer solution containing several different metal ions, viz., Na^+, Mg^{2+}, Ni^{2+}, and Cd^{2+} ions. In particular, the amount of V_{DP} shift on introducing Cu^{2+} ions at a concentration of 500 μM was about 10 times larger than that on introducing Na^+, Mg^{2+}, Ni^{2+}, and Cd^{2+} ions at the same concentration. Therefore, our results indicate that the TCA-immobilized G-FETs provide high sensitivity and selectivity for the detection of Cu^{2+} ions, making them promising candidates as portable Cu^{2+} sensors. Moreover, our research shows the importance of coordination structures between TCA and metal ions for the detection of specific metal ions using G-FETs. Moreover, in a manner similar to the approach followed in our study, other heavy metal ion sensors could be realized by adjusting the molecular structure to ensure the formation of a coordinate structure between the molecule and metal ions.

EXPERIMENTAL METHODS

Fabrication Process for G-FETs. First, monolayer graphene was synthesized on Cu foil (JX Nippon Mining & Metals, HA) via chemical vapor deposition. Before use, the Cu foil was annealed under a flow of 3% H_2 and 97% Ar at 500 sccm for 41 min to remove any native oxide so that Cu exhibits catalytic activity. Graphene was synthesized at 1035 °C by cracking CH_4 under both 3% H_2 and 97% Ar flow at 15 sccm, and 5% CH_4 and 95% Ar flow at 1500 sccm for 35 min. Next, the graphene was transferred onto a Si/SiO_2 substrate using poly(methyl methacrylate) (PMMA) and annealed at 330 °C for 1 h under a 3% H_2 and 97% Ar flow to remove impurities such as residual PMMA. Subsequently, Ni(10 nm) and Au(30 nm) were deposited as sources and drain electrodes via a photolithography technique. The channel distance and width for the source and drain were approximately 5 and 15 μm, respectively.[52]

Adsorption of TCA on Graphene and Measurement Methods. After G-FETs ware fabricated, a 50 μM solution was prepared by dissolving TCA (Tokyo Chemical Industry Co.) in chloroform. Then, the G-FETs were immersed in this prepared solution to immobilize TCA on graphene through $\pi-\pi$ interactions between them.[41,42] These G-FETs were then taken out of the solution and dried to obtain the required graphene-based sensors. Next, a silicon rubber pool was attached to the G-FETs so that the graphene channel could be immersed in a Tris-HCl buffer (20 mM, pH 8.0). A saturated Ag/AgCl electrode was used as the reference electrode.[53] NaCl, $MgCl^2$, $CdSO_4$, $NiSO_4$, and $CuSO_4$ solutions at various concentrations were added to the Tris-HCl buffer solution to increase the Na^+, Mg^{2+}, Cd^{2+}, Ni^{2+}, and Cu^{2+} concentrations in the reagent solution, respectively. The transfer characteristics of the G-FETs were measured by applying a drain voltage of 50

DOI: 10.1021/acsomega.9b03821
ACS Omega 2020, 5, 877−881

mV using a semiconductor parameter analyzer (Keysight Technologies, B2912).

AUTHOR INFORMATION

Corresponding Authors

*E-mail: ikuta@go.tuat.ac.jp (T.I.).
*E-mail: maehashi@cc.tuat.ac.jp (K.M.).

ORCID

Kenzo Maehashi: 0000-0002-9925-8874

Notes

The authors declare no competing financial interest.

ACKNOWLEDGMENTS

This research was partly supported by the Uehara Memorial Foundation and the Environment Research and Technology Development Fund (5RF-1802) of the Environmental Restoration and Conservation Agency of Japan and Grants-in-Aid for Scientific Research (B) (JP19H02582) and Challenging Research (Exploratory) (JP19K21963) from JSPS.

REFERENCES

(1) Singh, A.; Sharma, R. K.; Agrawal, M.; Marshall, F. M. Health risk assessment of heavy metals via dietary intake of foodstuffs from the wastewater irrigated site of a dry tropical area of India. *Food Chem. Toxicol.* **2010**, *48*, 611−619.

(2) Jang, A.; Seo, Y.; Bishop, P. L. The removal of heavy metals in urban runoff by sorption on mulch. *Environ. Pollut.* **2005**, *133*, 117−127.

(3) Turdean, G. L. Design and Development of Biosensors for the Detection of Heavy Metal Toxicity. *Int. J. Electrochem.* **2011**, *2011*, 1.

(4) Gao, C.; Yu, X.-Y.; Xiong, S.-Q.; Liu, J.-H.; Huang, X.-J. Electrochemical Detection of Arsenic(III) Completely Free from Noble Metal: Fe3O4 Microspheres-Room Temperature Ionic Liquid Composite Showing Better Performance than Gold. *Anal. Chem.* **2013**, *85*, 2673−2680.

(5) Valko, M.; Morris, H.; Cronin, M. Metals, Toxicity and Oxidative Stress. *Curr. Med. Chem.* **2005**, *12*, 1161−1208.

(6) Sumner, E. R.; Shanmuganathan, A.; Sideri, T. C.; Willetts, S. A.; Houghton, J. E.; Avery, S. V. Oxidative protein damage causes chromium toxicity in yeast. *Microbiology* **2005**, *151*, 1939−1948.

(7) Li, P.; Zhang, D.; Wu, J.; Cao, Y.; Wu, Z. Flexible integrated black phosphorus sensor arrays for high performance ion sensing. *Sens. Actuators, B* **2018**, *273*, 358−364.

(8) Steinnes, E. Atmospheric deposition of heavy metals in Norway studied by the analysis of moss samples using neutron activation analysis and atomic absorption spectrometry. *J. Radioanal. Chem.* **1980**, *58*, 387−391.

(9) Daşbaşı, T.; Saçmacı, Ş.; Ülgen, A.; Kartal, Ş. A solid phase extraction procedure for the determination of Cd(II) and Pb(II) ions in food and water samples by flame atomic absorption spectrometry. *Food Chem.* **2015**, *174*, 591−596.

(10) McComb, J. Q.; Rogers, C.; Han, F. X.; Tchounwou, P. B. Rapid Screening of Heavy Metals and Trace Elements in Environmental Samples Using Portable X-Ray Fluorescence Spectrometer, A Comparative Study. *Water, Air, Soil Pollut.* **2014**, *225*, 2169.

(11) Zhang, H.; Wang, Z.-Y.; Yang, X.; Zhao, H.-T.; Zhang, Y.-C.; Dong, A.-J.; Jing, J.; Wang, J. Determination of free amino acids and 18 elements in freeze-dried strawberry and blueberry fruit using an Amino Acid Analyzer and ICP-MS with micro-wave digestion. *Food Chem.* **2014**, *147*, 189−194.

(12) Veglio', F.; Beolchini, F. Removal of metals by biosorption: a review. *Hydrometallurgy* **1997**, *44*, 301−316.

(13) Lee, C.; Wei, X.; Kysar, J. W.; Hone, J. Measurement of the Elastic Properties and Intrinsic Strength of Monolayer Graphene. *Science* **2008**, *321*, 385.

(14) Balandin, A. A. Thermal properties of graphene and nanostructured carbon materials. *Nat. Mater.* **2011**, *10*, 569.

(15) Sakamoto, Y.; Uemura, K.; Ikuta, T.; Maehashi, K. Palladium configuration dependence of hydrogen detection sensitivity based on graphene FET for breath analysis. *Jpn. J. Appl. Phys.* **2018**, *57*, 04FP05.

(16) Nozaki, R.; Ikuta, T.; Ueno, K.; Tsukakoshi, K.; Ikebukuro, K.; Maehashi, K. Ethanol Detection at the Parts per Billion Level with Single-Stranded-DNA-Modified Graphene Field-Effect Transistors. *Phys. Status Solidi B* **2019**, *0*, 1900376.

(17) Hu, S.-K.; Lo, F.-Y.; Hsieh, C.-C.; Chao, L. Sensing Ability and Formation Criterion of Fluid Supported Lipid Bilayer Coated Graphene Field-Effect Transistors. *ACS Sens.* **2019**, *4*, 892−899.

(18) Okuda, S.; Ono, T.; Kanai, Y.; Ikuta, T.; Shimatani, M.; Ogawa, S.; Maehashi, K.; Inoue, K.; Matsumoto, K. Graphene Surface Acoustic Wave Sensor for Simultaneous Detection of Charge and Mass. *ACS Sens.* **2018**, *3*, 200−204.

(19) Li, P.; Liu, B.; Zhang, D.; Sun, Y. e.; Liu, J. Graphene field-effect transistors with tunable sensitivity for high performance Hg (II) sensing. *Appl. Phys. Lett.* **2016**, *109*, 153101.

(20) Ohno, Y.; Maehashi, K.; Inoue, K.; Matsumoto, K. Label-Free Aptamer-Based Immunoglobulin Sensors Using Graphene Field-Effect Transistors. *Jpn. J. Appl. Phys.* **2011**, *50*, 070120.

(21) Pumera, M. Graphene in biosensing. *Mater. Today* **2011**, *14*, 308−315.

(22) Tehrani, Z.; Burwell, G.; Azmi, M. A. M.; Castaing, A.; Rickman, R.; Almarashi, J.; Dunstan, P.; Beigi, A. M.; Doak, S. H.; Guy, O. J. Generic epitaxial graphene biosensors for ultrasensitive detection of cancer risk biomarker. *2D Materials* **2014**, *1*, 025004.

(23) Teixeira, S.; Conlan, R. S.; Guy, O. J.; Sales, M. G. F. Label-free human chorionic gonadotropin detection at picogram levels using oriented antibodies bound to graphene screen-printed electrodes. *J. Mater. Chem. B* **2014**, *2*, 1852−1865.

(24) Zeng, Q.; Cheng, J.; Tang, L.; Liu, X.; Liu, Y.; Li, J.; Jiang, J. Self-Assembled Graphene-Enzyme Hierarchical Nanostructures for Electrochemical Biosensing. *Adv. Funct. Mater.* **2010**, *20*, 3366−3372.

(25) Zeng, G.; Xing, Y.; Gao, J.; Wang, Z.; Zhang, X. Unconventional Layer-by-Layer Assembly of Graphene Multilayer Films for Enzyme-Based Glucose and Maltose Biosensing. *Langmuir* **2010**, *26*, 15022−15026.

(26) Ohno, Y.; Okamoto, S.; Maehashi, K.; Matsumoto, K. Direct Electrical Detection of DNA Hybridization Based on Electrolyte-Gated Graphene Field-Effect Transistor. *Jpn. J. Appl. Phys.* **2013**, *52*, 110107.

(27) Guo, Y.; Guo, S.; Ren, J.; Zhai, Y.; Dong, S.; Wang, E. Cyclodextrin Functionalized Graphene Nanosheets with High Supramolecular Recognition Capability: Synthesis and Host−Guest Inclusion for Enhanced Electrochemical Performance. *ACS Nano* **2010**, *4*, 4001−4010.

(28) Maehashi, K.; Sofue, Y.; Okamoto, S.; Ohno, Y.; Inoue, K.; Matsumoto, K. Selective ion sensors based on ionophore-modified graphene field-effect transistors. *Sens. Actuators, B* **2013**, *187*, 45−49.

(29) Campos, R.; Borme, J.; Guerreiro, J. R.; Machado, G.; Cerqueira, M. F.; Petrovykh, D. Y.; Alpuim, P. Attomolar Label-Free Detection of DNA Hybridization with Electrolyte-Gated Graphene Field-Effect Transistors. *ACS Sens.* **2019**, *4*, 286−293.

(30) Morohashi, N.; Narumi, F.; Iki, N.; Hattori, T.; Miyano, S. Thiacalixarenes. *Chem. Rev.* **2006**, *106*, 5291−5316.

(31) Iki, N.; Kabuto, C.; Fukushima, T.; Kumagai, H.; Takeya, H.; Miyanari, S.; Miyashi, T.; Miyano, S. Synthesis of p-tert-Butylthiacalix[4]arene and its Inclusion Property. *Tetrahedron* **2000**, *56*, 1437−1443.

(32) Shokova, E. A.; Kovalev, V. V. Thiacalixarenes-A New Class of Synthetic Receptors. *Russ. J. Org. Chem.* **2003**, *39*, 1−28.

(33) Sone, T.; Ohba, Y.; Moriya, K.; Kumada, H.; Ito, K. Synthesis and properties of sulfur-bridged analogs of p-tert-Butylcalix[4]arene. *Tetrahedron* **1997**, *53*, 10689−10698.

(34) Lhoták, P. Chemistry of Thiacalixarenes. *Eur. J. Org. Chem.* **2004**, *2004*, 1675−1692.

DOI: 10.1021/acsomega.9b03821
ACS Omega 2020, 5, 877−881

(35) Morohashi, N.; Iki, N.; Sugawara, A.; Miyano, S. Selective oxidation of thiacalix[4]arenes to the sulfinyl and sulfonyl counterparts and their complexation abilities toward metal ions as studied by solvent extraction. *Tetrahedron* **2001**, *57*, 5557−5563.
(36) Iki, N.; Morohashi, N.; Narumi, F.; Miyano, S. High Complexation Ability of Thiacalixarene with Transition Metal Ions. The Effects of Replacing Methylene Bridges of Tetra(p-t-butyl)-calix[4]arenetetrol by Epithio Groups. *Bull. Chem. Soc. Jpn.* **1998**, *71*, 1597−1603.
(37) Yushkova, E. A.; Stoikov, I. I. p-tert-Butyl Thiacalix[4]arenes Functionalized with Amide and Hydrazide Groups at the Lower Rim inCone,Partial Cone, and1,3-AlternateConformations Are "Smart" Building Blocks for Constructing Nanosized Structures with Metal Cations ofs-,p-, andd-Elements in the Organic Phase. *Langmuir* **2009**, *25*, 4919−4928.
(38) Evtugyn, G.; Stoikov, I.; Belyakova, S.; Stoikova, E.; Shamagsumova, R.; Zhukov, A.; Antipin, I.; Budnikov, H. Selectivity of solid-contact Ag potentiometric sensors based on thiacalix[4]arene derivatives. *Talanta* **2008**, *76*, 441−447.
(39) Modi, K.; Panchal, U.; Dey, S.; Patel, C.; Kongor, A.; Pandya, H. A.; Jain, V. K. Thiacalix[4]arene-tetra-(quinoline-8- sulfonate): a Sensitive and Selective Fluorescent Sensor for Co (II). *J. Fluoresc.* **2016**, *26*, 1729−1736.
(40) Kumar, R.; Lee, Y. O.; Bhalla, V.; Kumar, M.; Kim, J. S. Recent developments of thiacalixarene based molecular motifs. *Chem. Soc. Rev.* **2014**, *43*, 4824−4870.
(41) Zhang, J.; Podoprygorina, G.; Brusko, V.; Böhmer, V.; Janshoff, A. Functionalized Calix[8]arenes, Synthesis and Self-assembly on Graphite. *Chem. Mater.* **2005**, *17*, 2290−2297.
(42) Eroglu, E.; Zang, W.; Eggers, P. K.; Chen, X.; Boulos, R. A.; Wahid, M. H.; Smith, S. M.; Raston, C. L. Nitrate uptake by p-phosphonic acid calix[8]arene stabilized graphene. *Chem. Commun.* **2013**, *49*, 8172−8174.
(43) Sofue, Y.; Ohno, Y.; Maehashi, K.; Inoue, K.; Matsumoto, K. Highly Sensitive Electrical Detection of Sodium Ions Based on Graphene Field-Effect Transistors. *Jpn. J. Appl. Phys.* **2011**, *50*, 06GE07.
(44) Yang, L.; Zhao, H.; Li, Y.; Ran, X.; Deng, G.; Zhang, Y.; Ye, H.; Zhao, G.; Li, C.-P. Indicator displacement assay for cholesterol electrochemical sensing using a calix[6]arene functionalized graphene-modified electrode. *Analyst* **2016**, *141*, 270−278.
(45) Liu, L.; Zhang, K.; Wei, Y. A simple strategy for the detection of Cu(ii), Cd(ii) and Pb(ii) in water by a voltammetric sensor on a TC4A modified electrode. *New J. Chem.* **2019**, *43*, 1544−1550.
(46) Wang, L.; Wang, X.; Shi, G.; Peng, C.; Ding, Y. Thiacalixarene Covalently Functionalized Multiwalled Carbon Nanotubes as Chemically Modified Electrode Material for Detection of Ultratrace Pb2+ Ions. *Anal. Chem.* **2012**, *84*, 10560−10567.
(47) Pearson, R. G. Hard and Soft Acids and Bases. *J. Am. Chem. Soc.* **1963**, *85*, 3533−3539.
(48) Pearson, R. G. Hard and soft acids and bases, HSAB, part 1: Fundamental principles. *J. Chem. Educ.* **1968**, *45*, 581.
(49) Iki, N.; Kumagai, H.; Morohashi, N.; Ejima, K.; Hasegawa, M.; Miyanari, S.; Miyano, S. Selective oxidation of thiacalix[4]arenes to the sulfinyl- and sulfonylcalix[4]arenes and their coordination ability to metal ions. *Tetrahedron Lett.* **1998**, *39*, 7559−7562.
(50) Theophanides, T.; Anastassopoulou, J. Copper and carcinogenesis. *Crit. Rev. Oncol.-Hematol.* **2002**, *42*, 57−64.
(51) Swenson, D.; Baenziger, N. C.; Coucouvanis, D. Tetrahedral mercaptide complexes. Crystal and molecular structures of [(C6H5)-4P]2M(SC6H5)4 complexes (M = cadmium(II), zinc(II), nickel(II), cobalt(II), and manganese(II)). *J. Am. Chem. Soc.* **1978**, *100*, 1932−1934.
(52) Uemura, K.; Ikuta, T.; Maehashi, K. Turbostratic stacked CVD graphene for high-performance devices. *Jpn. J. Appl. Phys.* **2018**, *57*, 030311.
(53) Katsura, T.; Yamamoto, Y.; Maehashi, K.; Ohno, Y.; Matsumoto, K. High-Performance Carbon Nanotube Field-Effect Transistors with Local Electrolyte Gates. *Jpn. J. Appl. Phys.* **2008**, *47*, 2060−2063.

DOI: 10.1021/acsomega.9b03821
ACS Omega 2020, 5, 877−881